SAR comparison between CASL and pCASL at high magnetic field and evaluation of the benefit of a dedicated labeling coil

Hirschler, L.; Collomb, N.; Voiron, J.; Kohler, S.; Barbier, E.L.; Warnking, J.M.

Received: 14 February 2019 | Revised: 12 July 2019 | Accepted: 13 July 2019

DOI: 10.1002/mrm.27931

NOTE

Magnetic Resonance in Medicine

SAR comparison between CASL and pCASL at high magnetic field and evaluation of the benefit of a dedicated labeling coil

Lydiane Hirschler[1,2] | **Nora Collomb**[1,3] | **Jérôme Voiron**[2] | **Sascha Köhler**[2] | **Emmanuel L. Barbier**[1] | **Jan M. Warnking**[1]

[1]Univ. Grenoble Alpes, Inserm, U1216, Grenoble Institut Neurosciences, Grenoble, France

[2]Bruker BioSpin, Ettlingen, Germany

[3]Univ. Grenoble Alpes, Inserm, UMS017, CNRS, US3552, CHU Grenoble Alpes, IRMaGe, Grenoble, France

Correspondence
Jan M. Warnking, Grenoble Institut des Neurosciences, Chemin Fortuné Ferrini, 38700 La Tronche, France.
Email: jan.warnking@univ-grenoble-alpes.fr

Funding information
French National Research Agency Infrastructure d'avenir en Biologie Santé, Grant/Award Numbers: ANR-11-INBS-0006; NeuroCog IDEX UGA Investissements d'Avenir, Grant/Award Numbers: ANR-15-IDEX-02. French National Association of Research and Technology, CIFRE Grant.

Purpose: To investigate the heating induced by (pseudo)-continuous arterial spin labeling ((p)CASL) sequences in vivo at 9.4T and to evaluate the benefit of a dedicated labeling coil.

Methods: Temperature was measured continuously in the brain, neck, and rectum of 9 rats with fiber-optic temperature probes while running pCASL-EPI and CASL-EPI sequences, with labeling B_1 amplitudes (B_{1ave}) of 3, 5, and 7 μT and using a dedicated labeling RF coil or a volume coil. From the temperature time courses, the corresponding specific absorption rate (SAR) was computed. A trade-off between SAR and labeling quality was determined based on measured inversion efficiencies.

Results: ASL experiments with standard parameters (B_{1ave} = 5 μT, T_{acq} = 4 min, labeling with volume coil) lead to a brain temperature increase due to RF of 0.72 ± 0.46 K for pCASL and 0.25 ± 0.17 K for CASL. Using a dedicated labeling coil reduced the RF-induced SAR by a factor of 10 in the brain and a factor of 2 in the neck. Besides SAR due to RF, heat from the coil decoupling circuits produced significant temperature increases. When labeling with a dedicated coil, this mechanism was the dominant source of brain heating. At equivalent RF-SAR, CASL provided slightly superior label efficiency to pCASL and is therefore the preferred sequence when an ASL coil is available.

Conclusion: B_{1ave} = 4–5 μT provided a good compromise between label efficiency and SAR, both for pCASL and CASL. The sensitivity of animals to heating should be taken into account when optimizing preclinical ASL protocols and may require reducing scan duration or lowering B_{1ave}.

KEYWORDS
9.4T, arterial spin labeling (ASL), perfusion, rat, specific absorption rate (SAR)

1 | INTRODUCTION

Arterial spin labeling (ASL) enables repeated, non-invasive cerebral blood flow (CBF) measurements via MR. Its recommended implementation for clinical applications is pseudo-continuous ASL (pCASL).[1] In rodents, however, the use of continuous arterial spin labeling (CASL) or pulsed ASL[2] is more common, because pCASL is not a

commercially available technique on preclinical systems. An advantage of pCASL over CASL is that multi-slice acquisitions are straightforward, whereas multi-slice CASL requires the use of a dedicated labeling coil or special label and control RF pulses to avoid magnetization transfer (MT) effects. Compared to pulsed ASL, the long labeling periods in (p)CASL have the advantage of producing much higher ASL signal[3] and therefore facilitate CBF measurements. However, the long labeling RF pulse trains make (p)CASL prone to increased energy deposition in the imaged subject, especially at higher magnetic fields. Heating can not only lead to safety concerns,[4,5] but may also impact blood flow.[6,7] One way to reduce RF energy deposition is the use of a dedicated labeling coil located under the neck, to label blood in the nearby brain feeding arteries while limiting the size of the region exposed to RF magnetic fields during labeling.

Heating due to RF exposure is characterized by the specific absorption rate (SAR). The SAR distribution is not homogeneous in the sample or subject and depends on various parameters such as the sample's geometry, its dielectric properties and localization in the RF field, the RF coil's properties, and the MR field-strength. Furthermore, SAR depends on the applied labeling B_1 amplitude.

In this study, we assessed SAR in animals by measuring temperature increases in situ (i.e., by implanting fiber-optic temperature probes in the animal). This method is invasive, but it is robust, does not rely on any assumptions about the coil or system design, and takes into account all possible heating sources as well as the cooling effects of blood flow. We investigated the heating induced by CASL and pCASL sequences in vivo at 9.4T for different labeling B_1 amplitudes and evaluated the benefit of a dedicated labeling coil. Part of this work was presented previously.[8]

2 | METHODS

2.1 | Animals

Twelve male Sprague–Dawley rats (231 ± 29 g, Charles Rivers, France) were used. All experiments were approved by the local ethics committee and performed in full compliance with the guidelines of the European community (EUVD-86/609/EEC) for the care and use of the laboratory animals, under permits (380820 for EB and B3851610008 for experimental and animal care facilities). All procedures were conducted under isoflurane anesthesia (IsoFlo, Axience, France, 5% for induction, 2% for maintenance in air:O_2 80%:20%). Respiration rate, heart rate, and oxygen saturation were maintained within the following ranges: 40–60 breaths/min, 400–500 beats/min, and 98–100%, respectively. Hot water was circulated in the cradle under the animal to globally maintain body temperature. The rat's head and the neck were outside of the region heated by the cradle.

In 9 animals, heating induced by the MR scans was assessed. Temperature was continuously measured using 3 fiber-optic temperature probes (model FTP-LTF2-ST-10M, Photon Control, Burnaby, BC, Canada; diameter 650 μm; sampling frequency 10 Hz, precision ±0.05 K) implanted (1) inside the brain, (2) subcutaneously in the neck (near the labeling plane and carotids), and (3) in the rectum (Supporting Information Figure S1).

In 3 additional animals, the tradeoff between SAR and ASL signal amplitude was investigated by measuring the inversion efficiencies (IE) of the ASL sequences. In these animals, rectal temperature was monitored and maintained between 36 and 37°C.

2.2 | MR experiments

Experiments were performed on a horizontal 9.4T scanner (Bruker BioSpec, AVIII-HD), using 3 Bruker RF coils:

- a transmit–receive, actively decoupled quadrature volume coil (86 mm inner diameter) for imaging and labeling;
- a receive-only, actively decoupled, surface phased-array (4-channel) rat head coil; and
- a Bruker-prototype transmit-receive, actively decoupled, single loop ASL labeling coil (23 mm diameter) placed under the animal's throat for labeling.

To avoid repositioning the animal and to obtain comparable results, all 3 coils were present for all scans (i.e., the dedicated ASL coil was present even when labeling was performed with the volume coil) and the tooth bar was in the same position for all animals, which had similar ages and weights.

2.2.1 | Global description of the in vivo SAR measurements

Adjustments, baseline CASL CBF measurement, and anatomical scans were followed by 12 ASL scans with different parameters to assess tissue heating, each of them followed by a short CASL scan with fixed parameters to measure CBF ($CASL_{Perfusion}$, see Supporting Information) and a 8-min pause to allow for cool-down. Reproducibility and heating during a long pCASL sequence were evaluated with 2 additional ASL scans. Additional anatomical scans were performed to localize the brain and neck temperature probes. The entire session lasted ~350 min per animal, after which the rats were euthanized.

2.2.2 | Anatomical scans

FLASH scans were acquired to visualize the fiber-optic probe position in the neck (resolution 0.195 × 0.195 × 0.8 mm^3,

acquisition time T_{acq} = 31 s, 20 slices). Fiber-optic probe position in the brain was assessed via axial, sagittal, and coronal T_2-weighted (T_{2w}) TurboRARE images (resolution 0.137 × 0.137 × 0.8 mm^3, T_{acq} = 201 s, 30 slices).

2.2.3 | Heating during ASL scans

ASL experiments were performed both with CASL and pCASL sequences, using the volume coil (subscript "vol") and dedicated ASL coil (subscript "lab") for labeling, leading to 4 types of ASL sequences. For each of these sequences, mean B_1 amplitudes (B_{1ave}) of 3, 5, and 7 μT were applied during labeling, resulting in 12 individual ASL scans, performed in random order. RF power was turned off during the control experiment for the $CASL_{lab}$ and $pCASL_{lab}$ scans, because the ASL coil induced no MT effects in the imaged slice.

Labeling pulses were applied in the neck, at 2 cm from the isocenter, with a labeling duration of 3 s followed by a 300-ms post-labeling delay and a single-shot spin-echo echo-planar imaging (EPI) acquisition using volume transmit and surface array receive coils (TE/TR = 22/4000 ms, resolution 0.234 × 0.234 × 1 mm^3, 1 slice). Thirty pairs of label/control images were acquired within 4 min. pCASL labeling pulse trains consisted of 400-μs Hanning-window shaped RF pulses repeated every 800 μs.

2.2.4 | Reproducibility

The 3 and 5 μT $pCASL_{vol}$ scans were repeated at the end of the scanning session. The second 5 μT $pCASL_{vol}$ scan lasted 20 min (150 label/control pairs) to evaluate the temperature evolution during longer acquisitions.

2.2.5 | Inversion efficiency measurements

IE was measured in the carotids 5 mm downstream of the labeling plane with a flow-compensated, ASL-encoded FLASH sequence for each ASL labeling scheme, each coil setup and B_{1ave} values of 1.5, 3, 5, and 7 μT. Both label and control inter-pulse phases were optimized before the pCASL IE measurement.[9]

2.3 | Data processing

2.3.1 | B_{1RMS}

The RMS B_1 (B_{1RMS}) was calculated from the pulse program for each sequence and each applied B_{1ave} (Table 1). The EPI excitation and refocusing pulses were also taken into account, even though their contribution was small. For a given B_{1ave}, B_{1RMS} is 3 times higher for pCASL than for CASL because of the pulsed nature of the RF in pCASL. Because RF power was turned off during the control experiment when labeling with the ASL coil, the applied B_{1RMS} was 2 times lower in the $CASL_{lab}$ and $pCASL_{lab}$ scans compared to labeling with the volume coil.

2.3.2 | SAR

From the global temperature time courses spanning the entire experiment (Figure 1A), each individual, sequence-specific, temperature curve was extracted. Because the 8-min pause after each $CASL_{Perfusion}$ scan was usually not sufficient to return to equilibrium temperature, the constant and linear components of the temperature drift measured during a 3-min baseline immediately preceding each sequence was removed from that sequence. The apparent SAR (SAR_{app}) was calculated via

$$SAR_{app} = S_{scan} \cdot C_{tissue}, \quad (1)$$

where S_{scan} is the slope of the linear fit of the temperature evolution measured between 45 s and 225 s after sequence onset and C_{tissue} the specific heat capacity of tissue (3664 J/(kg × K)).[10]

To better interpret the local SAR_{app} data, it is useful to distinguish between the contribution of RF energy deposition, SAR_{RF}, which is proportional to B^2_{1RMS}, and a B_1-independent component, Q_{dec}, which corresponds to the extrapolation of the linear fit of SAR_{app} to $B^2_{1RMS} = 0$

TABLE 1 RMS B_1 (B_{1RMS}) for different labeling amplitudes B_{1ave}

Labeling B_{1ave}		$CASL_{lab}$	$pCASL_{lab}$	$CASL_{vol}$	$pCASL_{vol}$
0 μT (EPI only)	1 slice	0.2 μT	0.2 μT	0.2 μT	0.2 μT
	5 slices ($CASL_{perfusion}$)	0.5 μT	–	–	–
3 μT	1 slice	1.8 μT	3.2 μT	2.6 μT	4.5 μT
5 μT	1 slice	3.1 μT	5.3 μT	4.3 μT	7.5 μT
	5 slices ($CASL_{perfusion}$)	4.3 μT	–	–	–
7 μT	1 slice	4.3 μT	7.4 μT	6.1 μT	10.5 μT

B_{1RMS} values include labeling and EPI readout. The 5-slice $CASL_{Perfusion}$ scan was used to measure CBF after each ASL scan (Figure 1A).

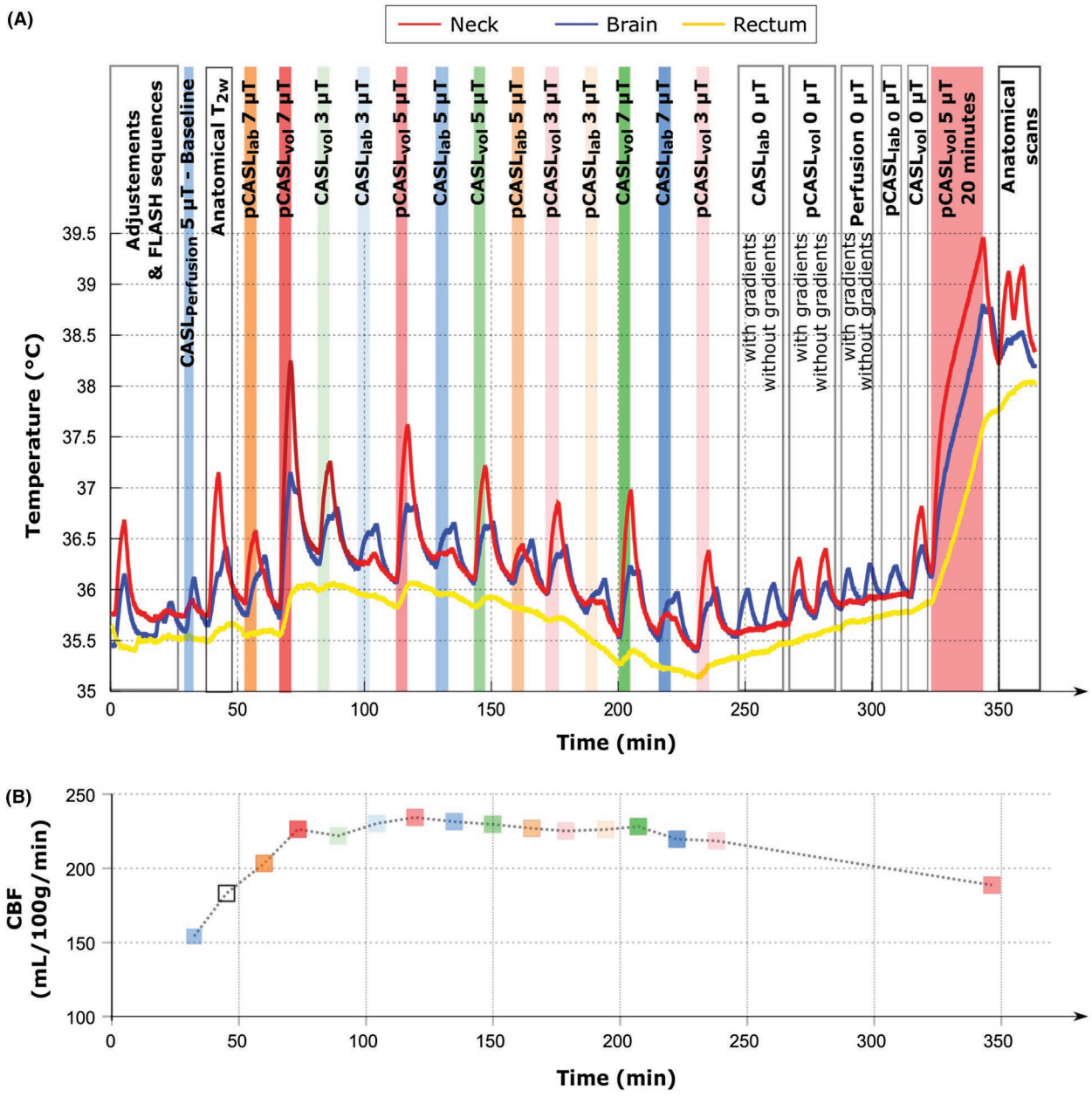

FIGURE 1 (A) Example of the temperature time courses measured at 3 different locations in 1 animal while performing ASL scans in 1 particular order: in the brain (blue), in the neck (red), and in the rectum (yellow). Note that the $CASL_{Perfusion}$ scans, repeated after each ASL scan to monitor CBF, have not been color-coded (cf. below), besides the first one (baseline). (B) CBF in mL/100 g/min across time measured after each sequence with $CASL_{Perfusion}$ for the rat shown in the first panel of this figure. The color code used for bars and boxes in (A) and (B) corresponds to the sequence type: the box is red for $pCASL_{vol}$, orange for $pCASL_{lab}$, green for $CASL_{vol}$, and blue for $CASL_{lab}$. The color saturation reflects the amplitude of B_{1ave}: the higher the saturation, the higher the applied B_{1ave}. In (B), the open box corresponds to the $CASL_{Perfusion}$ acquired after the anatomical T_{2w} scan

$$SAR_{app} = SAR_{RF} + Q_{dec} = SAR_{RF,rel} \cdot B_{1RMS}^2 + Q_{dec}, \quad (2)$$

where both SAR_{RF} and Q_{dec} have units of W/kg and the slope $SAR_{RF,rel}$ is in W/(kg × µT^2). We retrieved Q_{dec} and $SAR_{RF,rel}$ as the coefficients of the linear fit of SAR_{app} vs B_{1RMS}^2, for each animal, each probe, and each ASL sequence.

2.3.3 | IE quantification

IE was derived from the (p)CASL-FcFLASH data as follows

$$IE = \left| \frac{M_C - M_L}{2M_C} \right|, \quad (3)$$

where M_C and M_L are respectively the complex signals from the control and the label experiments. IE was averaged over

a manually drawn region of interest in each carotid. IE asymmetry was computed as the relative IE difference between the 2 carotids.

3 | RESULTS

3.1 | Global temperature and CBF time courses

Considerable temperature variations were observed in the brain and the neck, not only when acquiring ASL images, but also for anatomical imaging and while tuning and matching the quadrature volume coil (Figure 1A). The mean CBF (Figure 1B) was not following the temperature time course nor B^2_{1RMS} (Supporting Information Figure S5).

Even during the prolonged 20-min 5 μT $pCASL_{vol}$ scan, temperatures did not reach a plateau value: while the scan was running, temperatures increased, albeit at a reduced rate after ~7 min. In total, for this animal, this 20-min scan generated temperature increases of 3.3 K in the neck, 2.6 K in the brain, and 1.8 K in the rectum.

3.2 | In vivo SAR_{app} across sequences

The average SAR_{app} ($N = 9$ animals) as a function of B^2_{1RMS}, labeling coil, sequence type, and anatomical region is summarized in Figure 2. The SAR_{app} derived from the repeated 3-μT and 5-μT pCASL scans performed on each animal were comparable, with differences across animals of 0.5 ± 0.4 W/kg and 2 ± 2 W/kg, respectively, suggesting experimental stability. Here, and elsewhere in the manuscript, data are reported as mean ± SD. We did not add error bars in Figure 2 for sake of clarity. An inter-animal fluctuation was indeed present, because of variability in temperature probe placement (see Supporting Information).

As expected, SAR_{app} varied linearly with B^2_{1RMS}, with coefficients of determination R^2 of the linear fit above 0.9, except where SAR_{app} was independent of B^2_{1RMS} ($SAR_{RF,rel} \approx 0$). Global SAR_{app}, as measured via rectal temperature, was much lower for the dedicated ASL coil than for the volume coil (1.1 ± 0.7 W/kg vs. 5.5 ± 1.2 W/kg for pCASL, $B_{1ave} = 7$ μT).

3.3 | Heat induced in absence of RF emission

RF-independent heating (Q_{dec}) in the brain was independent of the labeling coil used and on the same order of magnitude as the SAR_{RF} deposited by label pulses applied with the volume RF coil. In the neck, only labeling with the volume coil produced significant Q_{dec}. More detailed investigation showed that Q_{dec} was due to heating from the coil decoupling circuits (see Supporting Information Figures S2 and S3).

3.4 | In vivo SAR_{RF}

If only SAR_{RF} is considered, pCASL and CASL heated in the same way at equal B^2_{1RMS} (Figure 3A,B), as expected, leading to 3 times higher SAR_{RF} for pCASL than for CASL at identical B_{1ave} and coil configuration.

The dedicated labeling coil deposited negligible RF energy in the brain (mean $SAR_{RF,rel} = 0.02$ W/(kg × μT²)) compared to the volume coil ($SAR_{RF,rel} = 0.19$ W/(kg × μT²)).

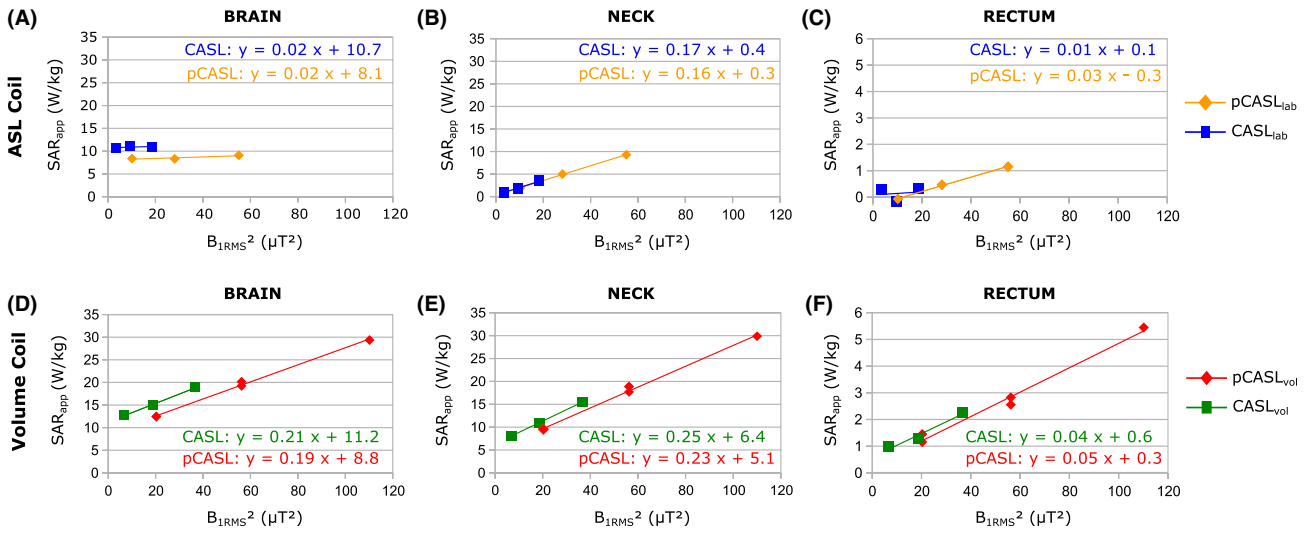

FIGURE 2 Average local SAR_{app} versus B^2_{1RMS} in the brain (A and D), in the neck (B and E), and in the rectum (C and F) for pCASL and CASL (mean across 9 animals). Labeling was performed either with the dedicated ASL labeling coil (A–C) or with the volume coil (D–F). For comparison, the anatomical T_2-TurboRARE scan led to a SAR_{app} of 13 W/kg in the brain, 15 W/kg in the neck, and 2 W/kg in the rectum. Lines represent a linear least-squares fit to the data. Reproducibility is shown by the superimposed red diamonds at $B^2_{1RMS} = 20$ μT² and at $B^2_{1RMS} = 56$ μT²

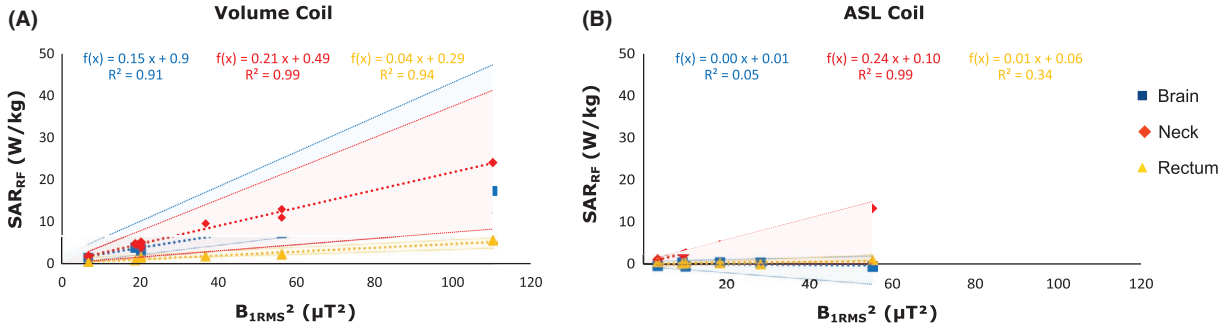

FIGURE 3 Average local SAR_{RF} versus B^2_{1RMS} for CASL and pCASL across animals in the brain (blue), the neck (red), and the rectum (yellow) for a labeling with the volume coil (A) or the dedicated ASL coil (B). Data from animals with the median $SAR_{RF,rel}$ are represented with markers. Linear fits to the data from animals with the median, maximum, and minimum $SAR_{RF,rel}$ are represented with dashed lines

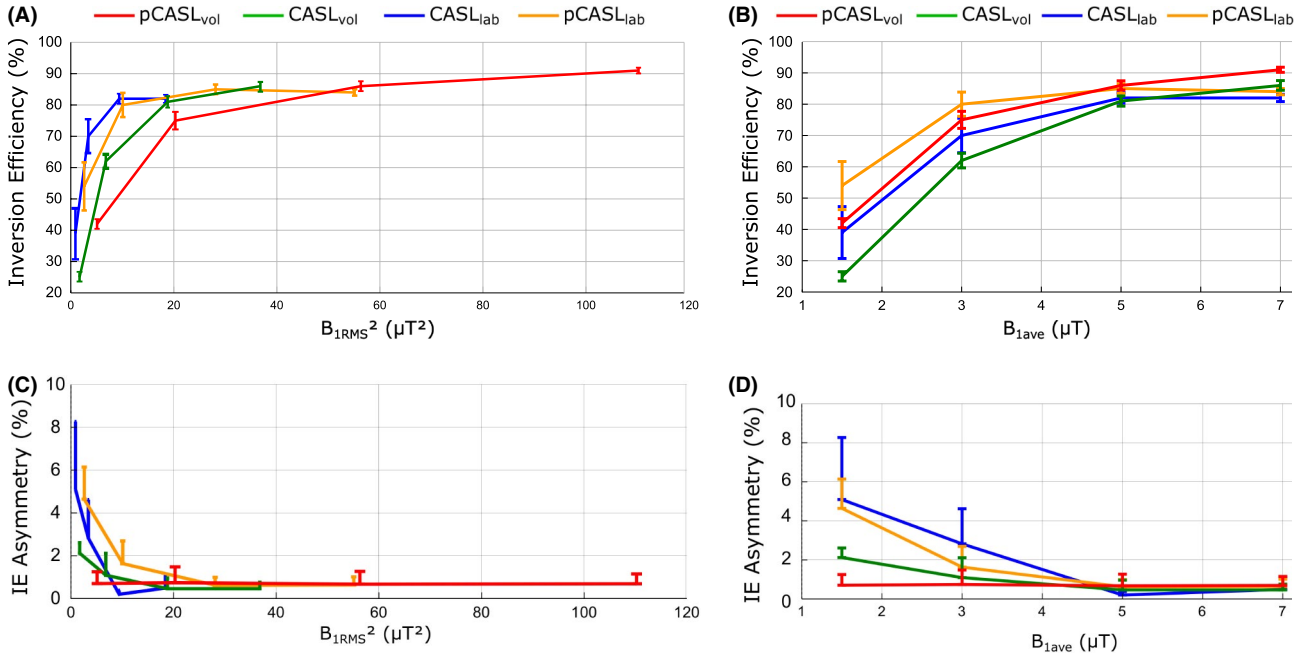

FIGURE 4 (A and B) Inversion efficiency (mean ± SD) and (C and D) IE asymmetry (mean ± SD) between carotids as a function of B^2_{1RMS} (A and C) and B_{1ave} (B and D). IE was measured 5 mm downstream of the labeling plane for $pCASL_{vol}$ (red), $CASL_{vol}$ (green), $CASL_{lab}$ (blue), and $pCASL_{lab}$(orange)

In the neck, labeling with a dedicated coil reduced the $SAR_{RF,rel}$ by 56 ± 7% compared to labeling with a volume coil, on average across all sequences and animals.

Temperature increase exclusively due to RF during the 4-min $pCASL_{vol}$ scans (B_{1ave} = 5 μT) was 0.72 ± 0.46 K in the brain with a range of 0.41–1.80 K across animals, and 0.87 ± 0.35 K in the neck (0.28–1.11 K), the variability being likely dominated by differences in temperature probe placement. When using a dedicated coil with CASL ($CASL_{lab}$, B_{1ave} = 5 μT), on average no temperature increase due to RF (0.00 ± 0.07 K) was observed in the brain, because of the small ASL coil coverage, and a slight RF heating of 0.12 ± 0.08 K was observed in the neck.

3.5 | Inversion efficiency

IE increased with B_{1ave} and therefore with B^2_{1RMS} (Figure 4A,B). Reducing B_{1ave} to <3 μT yielded low IE (<70%) for both $CASL_{vol}$ and $CASL_{lab}$ and asymmetrical labeling between carotids (Figure 4C,D), especially when labeling with the dedicated ASL coil. For B_{1ave} ≥5 μT, acceptable IE and low asymmetry were obtained for all sequences. Note that for both labeling coils, the pCASL sequence reached higher IE for given B_{1ave} values than the CASL methods. Still, because of the higher B^2_{1RMS} of pCASL, IE was slightly larger for CASL compared to pCASL for a given B^2_{1RMS} or SAR_{RF} (Figure 4A).

4 | DISCUSSION

This study investigated the heating induced by pCASL and CASL scans. We observed that the measured SAR_{app} was, as expected, due to the RF energy absorbed in the sample (SAR_{RF}) but also partly due to B_1-independent heating induced by the decoupling circuits of the coils used in this study (Q_{dec}), with which the animals were in contact.

A summary of the spatial distribution of the observed Q_{dec} and SAR_{RF} values is provided in the Supporting Information (Supporting Information Figure S4). A more detailed investigation of the spatial SAR distributions and detection of possible hot-spots would require MR thermography or electromagnetic simulations.

Our data show that heating during ASL sequences can be significant. It is therefore necessary to find a compromise B_{1ave} value that does not induce too much heat in the animals and still leads to sufficient and robust labeling efficiency. IE values increase with B_{1ave} and are in agreement with literature.[11] B_{1ave} amplitudes around 4–5 μT are good compromise values between IE (value and asymmetry) and SAR_{RF}. Using a dedicated ASL coil further reduces SAR while maintaining IE. Moreover, because CASL yields lower SAR_{RF} than pCASL at equal B_{1ave}, a $CASL_{lab}$ sequence with a B_{1ave} of 5 μT appears to be the best choice if an ASL coil is available. In this case, the SAR_{RF} is 0 ± 1 W/kg in the brain and 2 ± 1 W/kg in the neck (Figure 3; Supporting Information Table S1). If no ASL coil is available, labeling is necessarily performed with the volume-transmit coil and a pCASL sequence is the best option, despite the higher SAR_{RF} (11 ± 7 W/kg in the brain and 13 ± 5 W/kg in the neck), since $CASL_{vol}$ allows only a single-slice measurement because of MT effects. However, depending on the animal's condition, it may be necessary to adapt the pCASL scan duration, B_{1ave} amplitude, labeling duration, and/or the TR to reduce SAR to an acceptable value.[12] Decreasing transfer and increasing evacuation of heat from the RF coils, or choosing a receive coil with a position or implementation of the decoupling circuit that limits heating, may also significantly reduce power deposition compared to our observations. This may be an additional design criterion to consider in the development of RF coils for animals. In case of very stringent SAR constraints, pulsed ASL may be an alternative, albeit with lower SNR.

The observed IE asymmetries at lower B_{1ave}, especially when labeling with the ASL coil, are most probably due to the carotids position with respect to the labeling coil: at low B_{1ave}, the label pulse may not be adiabatic in one of the carotids, which leads to asymmetry. Asymmetry is observed both for CASL and pCASL, and therefore does not seem to be related to magnetic field heterogeneities.[9] Labeling with the volume coil reduces this asymmetry, which becomes negligible when increasing B_{1ave} for all coil configurations and sequences (Figure 4C,D). Given the reported SAR_{RF}, increasing B_{1ave} is recommended in case of IE asymmetry when labeling with the ASL coil.

Because of the heating localized around the head, with limited heat evacuation in the confined space of the MR scanner, the rectal temperature is lower compared to that of the brain during the major part of the experiment. Diseased animals (e.g., with stroke or traumatic brain injury) may have locally reduced CBF, resulting in restricted blood circulation and further reduced heat evacuation in the concerned regions. This could lead to higher temperature increases than the ones observed here, modify the animal's outcome, and thereby bias the results obtained.[4,5] Finally, because tissue relaxation times are affected by brain temperature, heating may affect studies investigating small changes in MRI signals during the imaging session.[13]

As guidance regarding the relative heating for different sequences in a given setup, it may be useful for the user to be informed by the scanner software of the B_{1RMS} of the sequences used.

5 | CONCLUSION

This study shows that ASL experiments with standard parameters (B_{1ave} = 3–7 μT) at 9.4T can lead to increase in tissue temperature. This should be taken into account, especially when using ASL sequences for long scanning. SAR can be dramatically reduced by using a dedicated ASL coil. A compromise must be found between SAR, inversion efficiency, acquisition time, and/or coil configuration.

ACKNOWLEDGMENTS

The authors acknowledge the excellent technical support of UMS-IRMaGe, partly funded by "Investissements d'Avenir" run by the French National Research Agency, grant "Infrastructure d'avenir en Biologie Santé" (ANR-11-INBS-0006). This project was partly funded by NeuroCog IDEX UGA ("Investissements d'Avenir" [ANR-15-IDEX-02]). Lydiane Hirschler's PhD was partly funded by the French National Association of Research and Technology via a CIFRE convention.

CONFLICT OF INTEREST

Lydiane Hirschler was paid by Bruker during her PhD. Jérôme Voiron and Sascha Köhler are Bruker employees.

ORCID

Lydiane Hirschler https://orcid.org/0000-0003-2379-0861
Emmanuel L. Barbier https://orcid.org/0000-0002-4952-1240
Jan M. Warnking https://orcid.org/0000-0002-1683-5163

REFERENCES

1. Alsop DC, Detre JA, Golay X, et al. Recommended implementation of arterial spin-labeled perfusion MRI for clinical applications: a consensus of the ISMRM perfusion study group and the European consortium for ASL in dementia. *Magn Reson Med*. 2015;73:102–116.
2. Nasrallah FA, Lee E, Chuang KH. Optimization of flow-sensitive alternating inversion recovery (FAIR) for perfusion functional MRI of rodent brain. *NMR Biomed*. 2012;25:1209–1216.
3. Chen Y, Wang D, Detre JA. Test-retest reliability of arterial spin labeling with common labeling strategies. *J Magn Reson Imaging*. 2011;33:940–949.
4. Mrozek S, Vardon F, Geeraerts T. Brain temperature: physiology and pathophysiology after brain injury. *Anesthesiol Res Pract*. 2012;2012.
5. Busto R, Dietrich WD, Globus M, Ginsberg MD. The importance of brain temperature in cerebral injury. *Stroke*. 1989;20:1113–1114.
6. Wang H, Wang B, Normoyle KP, et al. Brain temperature and its fundamental properties: a review for clinical neuroscientists. *Front Neurosci*. 2014;8:307.
7. Masuda H, Hirata A, Kawai H, et al. Local exposure of the rat cortex to radiofrequency electromagnetic fields increases local cerebral blood flow along with temperature. *J Appl Physiol*. 2011;110:142–148.
8. Hirschler L, Voiron J, Köhler S, Collomb N, Barbier EL, Warnking JM. SAR comparison between CASL and pCASL at high magnetic field (9.4T). Evaluation of the benefit of a separate labeling coil. In Proceedings of the 24th Annual Meeting of ISMRM, Singapore, 2016. Abstract 2748.
9. Hirschler L, Debacker CS, Voiron J, Köhler S, Warnking JM, Barbier EL. Interpulse phase corrections for unbalanced pseudo-continuous arterial spin labeling at high magnetic field. *Magn Reson Med*. 2018;79:1314–1324.
10. Sotero RC, Iturria-Medina Y. From blood oxygenation level dependent (BOLD) signals to brain temperature maps. *Bull Math Biol*. 2011;73:2731–2747.
11. Duhamel G, Callot V, Tachrount M, Alsop DC, Cozzone PJ. Pseudo-continuous arterial spin labeling at very high magnetic field (11.75 T) for high-resolution mouse brain perfusion imaging. *Magn Reson Med*. 2012;67:1225–1236.
12. Ghariq E, Teeuwisse WM, Webb AG, Van OM. Feasibility of pseudocontinuous arterial spin labeling at 7 T with whole-brain coverage. *MAGMA*. 2012;25:83–93.
13. Christie IN, Wells JA, Southern P, et al. fMRI response to blue light delivery in the naïve brain: Implications for combined optogenetic fMRI studies. *NeuroImage*. 2013;66:634–641.

SUPPORTING INFORMATION

Additional supporting information may be found online in the Supporting Information section at the end of the article.

FIGURE S1 Example of the temperature probe position in the brain (A) and in the neck (B). Top row: before installing the animal inside the MR scanner. Bottom row: T_2-TurboRARE (left) and FLASH (right) MR images. The red line corresponds to the probe

FIGURE S2 (A) Setup of coils and (B) corresponding illustrations with locations of the fiber-optic probes to measure temperature variations

FIGURE S3 Heating observed in absence of RF emission. (A) Images of the rat head coil (top row) and the ASL coil (bottom row) acquired with a thermal imaging camera at the end of 4-min pCASL and CASL scans. No RF power was emitted. The baseline temperature was 21°C. The cross and the red triangle indicate the warmest point for each applied sequence. (B) Illustrations of the array rat head coil (top row) and of the ASL coil (bottom row). Each number corresponds to a measurement position. (C) Heating (°/min) measured at the different coil locations is shown on (B) during pCASL and CASL scans

FIGURE S4 SAR induced in absence of RF emission (Q_{dec}, top row) and generated by the emitted RF field normalized to B_{1RMS}^2 (SAR_{RF}/B_{1RMS}^2, bottom row) in the brain (A, B, E, and F) and in the neck (C, D, G, and H) for pCASL. Each square represents the position of the fiber-optic probe of 1 particular animal. Note that the dark red squares on (A) and (B) represent values above the maximum of the color scale: $Q_{dec} = 38$ W/kg (A) and $Q_{dec} = 34$ W/kg (B). All other values are in the range of the color bars. The normalized SAR_{RF} values in (E)–(H) can be converted to the absolute SAR values for a given sequence by multiplying the scale on the color bars by the corresponding B_{1rms} as tabulated in Table 1

FIGURE S5 (A) Example of CBF maps in mL/100 g/min obtained with $CASL_{Perfusion}$. (B) Cortical CBF value measured with the $CASL_{Perfusion}$ scans (mean ± SEM across 5 animals) as a function of the B_{1RMS}^2 of the preceding heating scan

TABLE S1 Mean ± SD (9 animals) SAR_{RF} in W/kg across B_{1ave} for all sequences and temperature probes. The data in this table correspond to those displayed in Figure 3 (main document)

How to cite this article: Hirschler L, Collomb N, Voiron J, Köhler S, Barbier EL, Warnking JM. SAR comparison between CASL and pCASL at high magnetic field and evaluation of the benefit of a dedicated labeling coil. *Magn Reson Med*. 2020;83:254–261.
https://doi.org/10.1002/mrm.27931